

Rotational quenching of H_2CO by molecular hydrogen: cross-sections, rates, pressure broadening.

L. Wiesenfeld^{1*}, A. Faure¹

¹ *UJF-Grenoble 1/CNRS-INSU, Institut de Planétologie et d'Astrophysique de Grenoble (IPAG) UMR 5274, Grenoble F-38041, France*

Accepted xxx. Received xxxx; in original form 25 April 2013

ABSTRACT

We compute the rotational quenching rates of the first 81 rotational levels of ortho- and para- H_2CO in collision with ortho- and para- H_2 , for a temperature range of 10–300 K. We make use of the quantum close-coupling and coupled-states scattering methods combined with the high accuracy potential energy surface of Troscompt et al. (2009a). Rates are significantly different from the scaled rates of H_2CO in collision with He; consequently, critical densities are noticeably lower. We compare a full close-coupling computation of pressure broadening cross sections with experimental data and show that our results are compatible with the low temperature measurements of Mengel & De Lucia (2000), for a spin temperature of H_2 around 50 K.

Key words: Astrochemistry, molecular processes, molecular data, ISM: molecules

1 INTRODUCTION

In order to relate quantitatively the observed rotational spectra and the molecular abundances, knowledge of the relative importance of photon induced transitions and collision induced transitions is imperative. While the Einstein A and B coefficients can be obtained experimentally (see e.g. the JPL and CDMS databases Drouin (2012); Müller et al. (2005)), the rates of molecular collisional excitation/quenching need to be calculated with help of precise microscopic frameworks. Many molecular quenching rates have been put forward in the last 40 years, either for molecular collisions with He or for collisions with H, electrons and H_2 . In many types of interstellar regions, especially so when molecular complexity is present, the main collider is molecular hydrogen, H_2 . Recently, a renewed large effort has been devoted to compute the rotational quenching rates of molecules by H_2 (see references in the review by Van der Tak (2011)) and most collisional data are available in the BASECOL Dubernet et. al. (2012) and LAMDA Schöier et al. (2005) databases. Special emphasis was put on molecules specific to the Herschel Space Observatory, and among them, water. However, complex organic molecules continue to play a prominent role in the understanding of proto-stellar evolution as well as being probes for various interstellar environments.

Among all organic molecules, formaldehyde (H_2CO) is especially abundant, since it is the first stable molecule resulting from the hydrogenation of the ubiquitous CO

molecule (Peters et al. 2011). Being abundant and displaying a large range of both transition frequencies and energy levels, formaldehyde is a tool of choice to probe the physical conditions of the gaseous interstellar matter (Maret et al. 2004; Kama et al. 2013). By using models that do not suppose Local Thermodynamical Equilibrium (LTE), it is possible to reach reliable estimates of the molecular abundance of H_2CO together with the other parameters of the gas, its temperature and density (Ceccarelli et al. 2003; Van der Tak et al. 2007). **The famous formaldehyde “anomalous” absorption was also shown to provide a probe of the ortho-to-para ratio of H_2 (Troscompt et al. 2009b) and a distance-independent tracer of the cosmic star formation history (Darling & Zeiger 2012).**

Several computations of the excitation rates of H_2CO have been proposed in the literature. Excitation by He atoms, being easier to perform, has been used for long as a model for excitation by H_2 , even if it is known for being an underestimation of unknown precision (Green et al. 1978; Green 1991; Sharma et al. 2012). In our group, we computed (Troscompt et al. 2009a) the quenching rates of H_2CO by H_2 , but only for the low levels of excitation of ortho-formaldehyde (only the first 10 levels) and for low kinetic temperatures ($T \lesssim 100$ K). These computations were based on a high precision Potential Energy Surface (PES) for the van der Waals interaction $\text{H}_2\text{CO} - \text{H}_2$. In the present paper, we extend our previous computations to a much broader range of rotational energies and temperatures, for both ortho- and para- H_2CO , using the same PES. Also, in order to assess the precision of this PES, we compare experimental pressure broadening cross sections measured by

* E-mail : laurent.wiesenfeld@obs.ujf-grenoble.fr

Mengel & De Lucia (2000) to our own computations, in a manner similar to our recent works on the rotational excitation of H₂O and CO (Drouin & Wiesenfeld 2012b; Faure et al. 2013).

We organize the paper as follows. Section 2 describes the details of the scattering computation. Section 3 shows the results of our computations including cross sections, rates and pressure broadening. We end (section 4) with a discussion and a conclusion.

2 SCATTERING CALCULATIONS

As mentioned above, the PES for the interaction of H₂CO and H₂ has been described in our previous paper (Troscompt et al. 2009a). The PES was computed for frozen monomer geometries (rigid-rotor approximation). The geometries were those of the averaged distances and angles, at the ground vibrational state for both H₂CO and H₂. Using average ground state geometries instead of equilibrium geometries have been shown to give more reliable results (Valiron et al. 2008). **Since no modifications were performed on the PES, neither on the *ab initio* computations nor on the fits**, the reader is deferred to Troscompt et al. (2009a) for all necessary details of the *ab initio* and fitting procedures (see also Rist & Faure (2011) for the fitting procedure).

Both H₂CO and H₂ have each two identical ¹H nuclei, of nuclear spin 1/2. Hence, both exist in para and ortho spin states. For H₂, the para state (total nuclear spin $I = 0$) has even rotational states $J_2 = 0, 2, \dots$ (We denote by J_2 , the rotational quantum number of H₂). The ortho state ($I = 1$) on the opposite, has odd rotational states, $J_2 = 1, 3, \dots$. The H₂ rotational constant is taken at $B = 60.853 \text{ cm}^{-1}$. In the PES, the H-H distance is taken at $R = 1.448761 \text{ \AA}$, its average value at ground vibrational level (Troscompt et al. 2009a). The H₂CO molecule is an asymmetric rotor, with rotational constants (in cm^{-1}) : $A = 1.29543$, $B = 1.13419$, $C = 9.40552$ and centrifugal parameters $D_J = 0.251 \cdot 10^{-5}$, $D_{JK} = 0.431 \cdot 10^{-4}$, and $D_K = 0.648 \cdot 10^{-3}$. The rotational constant C is along the electric dipole, on the C_{2v} symmetry axis¹. Describing the rotational states by the usual $J_{K_A K_C}$ rotational (pseudo-)quantum numbers, para states ($I = 0$) of H₂CO correspond to K_A even and ortho states ($I = 1$) to K_A odd (the main quantum rotational number for H₂CO is denoted by J throughout this paper).

Scattering calculations were performed for all levels with a rotational energy $E_{\text{rot}} \leq 210 \text{ cm}^{-1}$, that is up to $J_{K_A K_C} = 10_{37}$ for ortho-H₂CO and $J_{K_A K_C} = 7_{44}$ for para-H₂CO. We computed the inelastic cross sections with a collision energy $1 \leq E_{\text{coll}} \leq 1000 \text{ cm}^{-1}$. This slightly extends the previous H₂CO-He computations of Green (1991) and extends our previous H₂CO-H₂ computations by an order of magnitude. Experimental (Bocquet et al. 1996) and computed para and ortho rotational levels of H₂CO are given in table 1, along with the level numbering used in the results. Note that restricting energies to $E \leq 210 \text{ cm}^{-1}$ entail $K_a \leq 4$. Also, for high enough J values, pairs of successive $K_A K_C$ and $K_A K_C + 1$ levels tend to be degenerate,

for all practical purposes. This degeneracy is all the more precise that the K_C values are small. Inspection of table 1 shows that the experimental - theoretical energy level differences ΔE are very small: $|\Delta E| \leq 0.43 \text{ cm}^{-1}$ (mean value $\langle |\Delta E| \rangle = 0.024 \text{ cm}^{-1}$).

All scattering calculations have been performed with the OpenMP version of the MOLSCAT code². The reduced mass for H₂CO-H₂ is 1.889053 amu. The coupled-channel (CC) and coupled-states (CS) equations were integrated using the diabatic modified log-derivative propagator.

The rotational basis set is devised as follows. For all scattering energies, if $J_{K_A K_C}$ is the last open channels, the $J' = J + 1, J + 2$ values were added to the basis. However, since a given J rotational number spans a large amount of rotational energy, rotational levels were capped, at $E_{\text{max}} = 400 \text{ cm}^{-1}$ for collision energies $E_{\text{tot}} \leq 175 \text{ cm}^{-1}$, and increasing progressively to $E_{\text{max}} = 1200 \text{ cm}^{-1}$ for $E_{\text{tot}} \sim 1000 \text{ cm}^{-1}$. **These large values of E_{max} are needed to converge cross sections; a similar effect was previously observed for methyl-formate colliding with Helium (Faure et al. 2011).**

The rotational basis for ortho-H₂ is $J_2 = 1$. It has been shown for many systems that including $J_2 = 3$ in the basis does not have a noticeable influence for temperatures as low as 300 K (e.g. Daniel, Dubernet & Grosjean (2011)). **The rotational basis for para-H₂ proved difficult to settle. We were able to use the $J_2 = 0, 2$ basis set for CC para-H₂ - ortho-H₂CO collisions, with $E_{\text{tot}} \leq 130 \text{ cm}^{-1}$ (Troscompt et al. 2009a). For para-H₂CO, because of the level structure, the $J_2 = 0, 2$ basis for CC computations proved to be practically impossible for $E_{\text{tot}} \gtrsim 50 \text{ cm}^{-1}$. As a result, we resorted only to a $J_2 = 0$ basis, both for ortho- and para-H₂CO, stretching the CC computations as high as possible and continuing with the CS approximation. In order to assess the importance of the $J_2 = 2$ channel, however, we complemented the ortho-H₂CO data with a full CS $J_2 = 0, 2$ computation up to $E_{\text{tot}} \sim 900 \text{ cm}^{-1}$, using a coarse energy grid. This allowed us to check *i*) that cross sections for transitions with $J_2 = 2 \rightarrow 0$ are negligible, *ii*) that cross sections for transitions with $J_2 = 2 \rightarrow 2$ are very similar to those with $J_2 = 1 \rightarrow 1$ (as observed for other systems, see e.g. Daniel, Dubernet & Grosjean (2011)) and *iii*) that the difference between the basis sets $J_2 = 0$ and $J_2 = 0, 2$ decreases with increasing collision energy, from an average of $\sim 30 \%$ to below 10% .**

Because of the large number of expansion terms of the potential function in the spherical harmonic basis (Troscompt et al. 2009a), several strategies have been devised in order to converge the inelastic scattering computations in a reasonable amount of time (We arbitrarily tried to limit ourselves to 72 hours of clock time, for one energy scattering point, on 12 CPU cores). The radial propagation used a step size parameter STEPS = 15 except at collision energies below 10 cm^{-1} where was STEPS progressively increased up to 50. Also, RMAX values were progressively increased in the

¹ This is the MOLSCAT convention, differing from usual spectroscopic conventions by the ordering of the axes.

² Repository at <http://ipag.osug.fr/~afaure/molscat/index.html>

low-energy regime from default to 100. Other propagation parameters were taken as the MOLSCAT default values.

For total energies above approximately 330 cm^{-1} the coupled channels (CC) approach, exact in the fully converged limit, proved to be impractical. We thus had to resort to the usual coupled states (CS) approximation, with all its shortcomings. Like in our recent HDO-H₂ rate calculations (Wiesenfeld, Scribano & Faure 2011), we used an additive constant to scale appropriately the CS cross sections by their counterpart CC values. Overlap of the CC and CS calculations showed the validity of these corrections. **The statistics of difference δ between the CC and CS cross-sections was also examined. We found the following values (in \AA^2 , s , the standard deviation): $\langle |\delta| \rangle \leq 0.5$, $s(\delta) \leq 2$.** Also, for collisions with ortho-H₂, the total angular momentum J_{tot} was not stepped by unit values, as is done usually. For CC calculation above $E_{\text{coll}} > 200 \text{ cm}^{-1}$, a step in J_{tot} value $J_{\text{STEP}} = 4$ was used, with a careful checking of the convergence of the $J_{\text{STEP}} > 1$ procedure. This procedure was used throughout the CS computations.

The energy grid was chosen to guarantee a good description of the resonances, including those pertaining to the high lying rotational states. Also, since we aim at rates for temperatures up to 300 K, a particular care was taken to ensure both some economy in the computational load and a good convergence of the rate computation. Let us recall that the quenching rate from state i to state j , $k_{j \leftarrow i}(T)$ (in $\text{cm}^3 \text{sec}^{-1}$) is related to the inelastic cross section $\sigma_{j \leftarrow i}(E)$ (in \AA^2 , with E , the collision energy) by the well known Boltzmann average :

$$k_{j \leftarrow i}(T) = \sqrt{\frac{8}{\pi \mu}} \frac{1}{T^3} \int_0^\infty \sigma_{j \leftarrow i}(E) E \exp(-E/T) dE, \quad (1)$$

where T and E are expressed in the same units, and μ is the collisional reduced mass. The probability density $E \exp(-E/T)$ going very slowly down with energy, it is customary, for calculating $k_{j \leftarrow i}(T = T_0)$, to compute $\sigma_{j \leftarrow i}(E)$ up to $E \sim 10 T_0$ (e.g., Dubernet et al. (2009)). This approach is prohibitively time-intensive for a heavy molecule like H₂CO, even within the CS approximation. For high lying rotational states, we inspected carefully the actual numerical convergence of equation 1 and stopped our energy grid as soon as the rate was saturated by 10% in general, and 25% for the highest levels, with $E_{\text{up}} > 150 \text{ cm}^{-1}$.

The computation of the pressure broadening cross-sections (Wiesenfeld & Faure 2010; Drouin & Wiesenfeld 2012b) necessitates a very fine energy grid and a good control of the elastic cross sections, much more difficult to obtain than the corresponding inelastic sections. Hence, we had to re-calculate all the S -matrices with collision energies from 2 to 70 cm^{-1} . Then, we compute the $\sigma^{\text{PB}}(T)$ in order to compare it with the experimental results of Mengel & De Lucia (2000), in a temperature range of 10 – 30 K. Both collisions with para-H₂ (basis set, $J_2 = 0, 2$) and ortho-H₂ (basis set, $J_2 = 1$) were performed on an identical fine energy grid **and in the CC formalism**.

3 RESULTS AND DISCUSSION

3.1 Cross sections

The inelastic cross sections have a general shape that is similar to all earlier findings, for collisions of a molecule with H₂. As usual, the inelastic scattering with $J_2 = 0$ may be markedly different from the scattering with $J_2 > 0$. This was observed and thoroughly discussed for H₂O and HDO scattering computations (Dubernet et al. 2009; Daniel, Dubernet & Grosjean 2011; Wiesenfeld, Scribano & Faure 2011; Faure et al. 2012), and observed for a wide range of other collisions, SO₂ and Cl atoms being recent examples (Cernicharo et al. 2011; Lique & Alexander 2012). Experiments with H₂ colliding with water molecules also extensively confirm this difference (Drouin & Wiesenfeld 2012b; Yang et al. 2011). The situation with formaldehyde colliding with H₂, $J_2 = 0$ and $J_2 > 0$ is however less clear, as some ortho-H₂ and para-H₂ collisions are nearly identical, especially for small sections and large ΔJ . Examples of astrophysical significative cross-sections $\sigma(E_{\text{coll}})$ are given in figure 4. Those three cases are representative of all these astrophysically relevant types of sections that we examined: $\sigma(E_{\text{tot}}; J_2 = 0) \ll \sigma(E_{\text{tot}}; J_2 > 0)$ even if the $\sigma(E_{\text{tot}}; J_2 = 0)$ displays a richer resonance structure, because of the disappearance of the supplementary quantum coupling $\mathbf{J} + \mathbf{J}_2 = \mathbf{J}_{12}$. In each case, we observe that $\sigma(E_{\text{coll}}; J_2 = 1) \simeq \sigma(E_{\text{coll}}; J_2 = 2)$, in structure and magnitude. Remember, however, that the threshold for scattering with $J_2 = 2$ is $B(\text{H}_2) \times 4 = 243.4 \text{ cm}^{-1}$ higher than for $J_2 = 1$. A full and reliable computation of H₂CO scattering with para-H₂, $J_2 \geq 2$ is thus impossible for all practical purposes, in the present computer configurations.

3.2 Rates

All quenching rates for all levels of table 1 are computed for the same temperature grid as Green (1991), $10 \text{ K} \leq T \leq 300 \text{ K}$. The full table is deposited in the LAMDA database (Schöier et al. 2005) and BASECOL database (Dubernet et al. 2012), and may be asked to the authors. The rates with ortho-H₂ are based on the $J_2 = 1$ sections only. In all cases, rates with para-H₂ are given as a Boltzman average over the populations of $J_2 = 0, 2$, with the further approximation of $\sigma(E_{\text{coll}}; J_2 = 2) \simeq \sigma(E_{\text{coll}}; J_2 = 1)$, when necessary (see above). The influence of the $J_2 = 2$ initial states may indeed be very large, as was also observed, in another context, for the pressure broadening of H₂O by H₂ (Drouin & Wiesenfeld 2012b).

Figure 4 compares globally present critical densities and critical densities from Green (1991), for electric-dipole allowed transitions. We compare our present rates with para-H₂ with the properly scaled rates with He. We have the following definition on the critical density n^* :

$$n_i^* = \frac{\sum_{j' < i} A_{j' \leftarrow i}}{\sum_{j < i} k_{j \leftarrow i}(T)} \quad (2)$$

where i is the level under scrutiny and j' denotes all levels connected by a radiative transition, while j spans all levels. Left panel shows the scatter of critical densities ratios at $T = 300 \text{ K}$, while on the right panel, all ratios are averaged and plotted against temperature. The scatter is moderate, with no ratio exceeding 3. The right panels shows the evolution of

Table 1. H₂CO rotational levels, in cm⁻¹. The experimental values are from Bocquet et al. (1996); the MOLSCAT values are calculated via the rotational constants described in the text.

Level	J	K_A	Para H ₂ CO		Experimental	Level	J	K_A	Ortho H ₂ CO		Experimental
			K_C	MOLSCAT					K_C	MOLSCAT	
1	0	0	0	0.00000	0.00000	1	1	1	1	10.53897	10.53900
2	1	0	1	2.42961	2.42960	2	1	1	0	10.70021	10.70010
3	2	0	2	7.28640	7.28640	3	2	1	2	15.23672	15.23690
4	3	0	3	14.56547	14.56550	4	2	1	1	15.72044	15.72020
5	4	0	4	24.25953	24.25970	5	3	1	3	22.28172	22.28220
6	5	0	5	36.35891	36.35920	6	3	1	2	23.24914	23.24870
7	2	2	1	40.04024	40.04020	7	4	1	4	31.67205	31.67290
8	2	2	0	40.04262	40.04260	8	4	1	3	33.28429	33.28350
9	3	2	2	47.32780	47.32780	9	5	1	5	43.40518	43.40670
10	3	2	1	47.33970	47.33970	10	5	1	4	45.82316	45.82200
11	6	0	6	50.85168	50.85240	11	6	1	6	57.47805	57.48040
12	4	2	3	57.04241	57.04250	12	6	1	5	60.86224	60.86050
13	4	2	2	57.07810	57.07800	13	7	1	7	73.88710	73.89070
14	7	0	7	67.72387	67.72520	14	7	1	6	78.39720	78.39490
15	5	2	4	69.18225	69.18240	15	3	3	1	88.23817	88.23820
16	5	2	3	69.26541	69.26520	16	3	3	0	88.23819	88.23830
17	6	2	5	83.74502	83.74530	17	8	1	8	92.62834	92.63370
18	6	2	4	83.91097	83.91060	18	4	3	2	97.95762	97.95760
19	8	0	8	86.95982	86.96210	19	4	3	1	97.95777	97.95780
20	7	2	6	100.72797	100.72860	20	8	1	7	98.42283	98.41970
21	7	2	5	101.02562	101.02500	21	5	3	3	110.10856	110.10860
22	9	0	9	108.54265	108.54640	22	5	3	2	110.10917	110.10920
23	8	2	7	120.12792	120.12910	23	9	1	9	113.69738	113.70500
24	8	2	6	120.62140	120.62030	24	9	1	8	120.93290	120.92900
25	10	0	10	132.45497	132.46091	25	6	3	4	124.69196	124.69200
26	9	2	8	141.94120	141.94321	26	6	3	3	124.69380	124.69380
27	9	2	7	142.71099	142.70931	27	10	1	10	137.08956	137.10020
28	4	4	0	155.16894	155.16940	28	7	3	5	141.70886	141.70889
29	4	4	1	155.16894	155.16940	29	7	3	4	141.71348	141.71350
30	11	0	11	158.67956	158.68851	30	10	1	9	145.92017	145.91530
31	10	2	9	166.16374	166.16690	31	8	3	6	161.16034	161.16051
32	10	2	8	167.30709	167.30440	32	8	3	5	161.17049	161.17059
33	5	4	1	167.31421	167.31461	33	11	1	11	162.79999	162.81450
34	5	4	2	167.31421	167.31461	34	11	1	10	173.37619	173.37041
35	6	4	2	181.88960	181.88989	35	9	3	7	183.04741	183.04781
36	6	4	3	181.88961	181.88989	36	9	3	6	183.06768	183.06790
37	12	0	12	187.20017	187.21330	37	12	1	12	190.82361	190.84309
38	11	2	10	192.79099	192.79581	38	12	1	11	203.29127	203.28461
39	11	2	9	194.42165	194.41750	39	10	3	8	207.37096	207.37180
40	7	4	3	198.89572	198.89600	40	10	3	7	207.40854	207.40891
41	7	4	4	198.89574	198.89600						

the average $\langle n_i^* \rangle$ as a function of T . For higher temperatures, the effect of H₂ being different of He diminishes, since higher collisions energies are more sensitive to the hard walls of the target, where the potential grows exponentially (repulsion of the wave functions). H₂ and He become more similar, and the rates tend one towards the other.

3.3 Pressure broadening

In order to assess the reliability of the PES, we found it useful to compare measured and computed pressure-broadening cross sections, $\sigma^{\text{PB}}(T)$ (Wiesenfeld & Faure 2010; Drouin & Wiesenfeld 2012b; Faure et al. 2013). The main advantage of pressure broadening is that experiments and computations held both absolute quantities, with no scaling involved, rendering the comparison very meaningful. Unfortunately, only a

very limited set of H₂CO pressure broadening data exists for an H₂ buffer gas (Mengel & De Lucia 2000), for very low temperatures. The experimental results for the 2₁₂ → 3₁₃ transition are depicted in figure 3, along with full CC calculations of $\sigma^{\text{PB}}(T)$. We see that the para-H₂ and ortho-H₂ computation bracket the experimental values, which are very well simulated by an ortho- to para-H₂ ratio (OPR) corresponding to a pseudo-equilibrium at ~ 50 K, **corresponding to a OPR of 0.27**. That the OPR of H₂ may vary during the collisional cooling experiment has been proved with cell walls covered with amorphous water (Drouin & Wiesenfeld 2012b). Nothing is known for formaldehyde, and discussion with the authors of Mengel & De Lucia (2000) could not settle the case. We remain thus with a good plausibility argument, as long as the pressure broadening experiments with H₂ are not fully characterized.

4 DISCUSSION - CONCLUSION

It is important to know which errors are to be expected, and to have some clues on how these errors might influence astrophysical modeling. We expect the error on the rates $k(T)$ to be uniformly increasing from low lying levels to higher lying ones, and also from low temperature to high temperature. Quantifying this error is very risky, as errors may arise from all the phases of the rate computation: *ab initio* computation, fits and long distance behavior of the PES, convergence of the CC/CS procedures, convergence of the averaging procedure of the sections with collision energy.

Internal consistency with our earlier approach (Troscompt et al. 2009a) show differences less than 10 %, for $J \leq 5$, $T \leq 50$ K. This shows that the convergence error in this domain cannot exceed 20-30%. In the high temperature domain ($T \geq 150$ K), it is safe to assume errors much larger than 30%, because of the poor convergence of formula (1), but still within a factor 2. The magnitude of the δ values as well as the similarities between the $J_2 = 1 \rightarrow 1$ and $J_2 = 2 \rightarrow 2$ plead in favor of such a conservative value, as does the convergence of critical densities between our work and the previous collisions with He by Green (1991).

Accuracy of the PES is very difficult to assess, without any firm experimental comparison, like has been done for H₂O and to a lesser extent CO (Yang et al. 2011; Drouin & Wiesenfeld 2012b; Faure et al. 2013; Chefdeville et al. 2012). Our results are, however, compatible with measurements of Mengel & De Lucia (2000). Because of the great importance and ubiquity of the formaldehyde molecule, further experiments would give indications on the precision of the PES and convergence procedures used in this paper.

The relevance of the ortho-to-para ratio of H₂ has been stressed several times already, as it may be of crucial importance in order to correctly model the astrophysical environments. While the difference in rates for ortho-H₂ and para-H₂ is large for low lying levels at low energies, see Troscompt et al. (2009b) for an application, this difference decreases at larger transition energies, as the hard walls of the PES play a more important role than the long range behavior. Indeed, the main increase in $\sigma(J_2 > 0)$ with respect to $\sigma(J_2 = 0)$ is due to the averaging out of the quadrupolar moment and dipolar polarizability of H₂ in its ground rotational states. The same is true, up to a global scale, for the difference in behavior between He and ortho-H₂.

Extension of these computations to higher levels and higher temperatures is by no means a difficult task, on the physics point of view, because of the rigid rotor structure of H₂CO, its first bending frequency (the out-of-plane bend) arising at 1167.3 cm⁻¹ (Clouthier & Ramsay 1983). The true limiting factor arises from numerical load, with very large $N \times N$ matrices to invert and propagate ($N > 2000$). The same situation arises for the excitation of heavier complex organic molecules, like methyl formate or dimethyl ether, which display many spectral lines very far from LTE, in various spectral surveys like Caux et al. (2011). Unfortunately, quasi classical trajectories methods are limited for all those cases because of ambiguities arising in the subsequent quantization of rotational levels (Faure & Wiesenfeld 2004). Use of very large grid of computers and combinations

of OpenMP/MPI approaches may overcome these difficulties.

We have calculated an extensive set of low to medium temperature quenching rates, for all levels of H₂CO below 210 cm⁻¹. These rates are ready to be incorporated in the various non-LTE models for the interstellar medium. At low temperatures, differences with earlier rates of H₂CO colliding with Helium are very important and they remain noticeable at all temperatures, with ratios up to 50% at 300 K, where they are the most similar. Since Troscompt et al. (2009a) was tailored to be very precise at low temperatures for ortho-H₂CO, we still recommend to use those rates for applications at $T \leq 30$ K. The present rates should have a large importance on the inferring of H₂CO column densities, away from LTE conditions.

ACKNOWLEDGMENTS

Many discussions with C. Ceccarelli and members of the CHESS team are gratefully acknowledged. The authors thank generous funding through the ANR and the CNES agencies, thanks to the FORCOMS contract (ANR-08-BLAN-022) and the CHESS Herschel Space Observatory Key Program funding. This work was also supported by the CNRS-INSU national program “Physique et Chimie du Milieu Interstellaire”. All calculations presented in this paper were performed at the “Service Commun de Calcul Intensif de l’Observatoire de Grenoble (SCCI)”.

REFERENCES

- Bocquet et al. 1996 J. Mol. Spec. 177, 154
- Caux E. et al. 2011 A&A 532, A23
- Ceccarelli, C., Maret, S., Tielens, A. G. G. M., Castets, A., & Caux, E. 2003, A&A, 410, 587
- Cernicharo, F. et al. 2011 A&A 531, A103
- Chefdeville S., Stoecklin T., Bergeat A., Hickson K.M., Naulin C., and Costes M. 2012 Phys. Rev. Lett. 109, 023201
- Clouthier D J , and Ramsay D A 1983, Annual Review of Physical Chemistry 34, 31
- Daniel F., Dubernet M.-L., and Grosjean A., 2011 A&A 536, A76
- Darling J., Zeiger B., 2012, ApJ, 749, L33
- Drouin, B. 2012, Molecular Spectroscopy : <http://spec.jpl.nasa.gov/ftp/pub/catalog/catdir.html>
- Drouin, B. and Wiesenfeld, L. 2012b, Phys. Rev. A 86, 022705
- Dubernet M.-L. and Grosjean A. 2002 A&A 390, 793
- Dubernet M.-L., Daniel F., Grosjean A., and Lin C.Y. 2009 A&A 497, 911
- M.L. Dubernet et al, "BASECOL2012: A Collisional Database Repository and Web Service within VAMDC", submitted to A. & A., 2012
- Faure A. and Wiesenfeld L. 2004 J. Chem. Phys. 121 6771

- Faure, A., Szalewicz, K., and Wiesenfeld, L. 2011, *J. Chem. Phys.*, 135, 024301.
- Faure, A., Wiesenfeld, L., Scribano Y., and Ceccarelli C. 2012, *MNRAS*, 420, 699
- Faure A., Wiesenfeld L., Drouin B., and Tennyson J., 2013, *J. Quant. Spectrosc. Radiat.*, 116, 79
- Green, S. , Garrison, B.J., Lester, W.A. Jr, and Miller, W.H., 1978, *ApJS*, 37, 321
- Green, S. 1991 *ApJS*, 76, 979
- Lique, F. and Alexander, M.H. 2012 *J. Chem. Phys.* 136, 124312
- Kama, M., López-Sepulcre, A., Dominik, C., Ceccarelli, C., Fuente, A., Caux, E., Higgins, R., Tielens, A.G.G.M., and Alonso-Albi, T. , submitted to *A&A* 2013.
- Maret, S., Ceccarelli, C., Caux, E., et al. 2004, *A &A*, 416, 577
- Mengel, M. and De Lucia, F.C. 2000, *ApJ*, 543, 271.
- Müller H. S. P. , Schlöder F. , Stutzki J., and Winnewisser G. 2005, *J. Mol. Struct.* 742, 215 : <http://www.astro.uni-koeln.de/cdms>
- Peters, P. et al. 2011, *J. Phys. Chem. A*, 115, 8983
- Rist C. and Faure A. 2011 *J. Mathematical Chemistry* 50, 588.
- Schöier, F.L. ,van der Tak, F.F.S., van Dishoeck E.F., Black, J.H. 2005, *A&A* 432, 369
- Sharma Monika, Sharma M.K., and Chandra Suresh, 2012, *Journal of Quantitative Spectroscopy & Radiative Transfer* 113 1898.
- Troscourt N., Faure A., Wiesenfeld L., Ceccarelli C., and Valiron P. 2009a, *A&A*, 493, 687
- Troscourt N., Faure A., Maret S., Ceccarelli C., Hily-Blant P., and Wiesenfeld L. 2009b, *A&A* 506, 1243
- Valiron P. et al., 2008, *J. Chem. Phys.* 129, 134306
- Van der Tak F.F.S., Black J.H., Schier F.L., Jansen D.J., van Dishoeck E.F. 2007, *A&A* 468, 627
- Van der Tak, F. 2011, *IAU Symposium* 280, *Radiative Transfer and Molecular Data for Astrochemistry*, pp 449–460.
- Wiesenfeld L. and Faure A., 2010, *Phys. Rev. A* 82, 040702(R)
- Wiesenfeld L., Scribano Y., and Faure A. 2011, *Phys.Chem.Chem.Phys.*, 13, 8230
- Yang, C.H., Sarma G., Parker D.H., ter Meulen, J.J., and L. Wiesenfeld, 2011, *J. Chem. Phys.* , 134, 204308

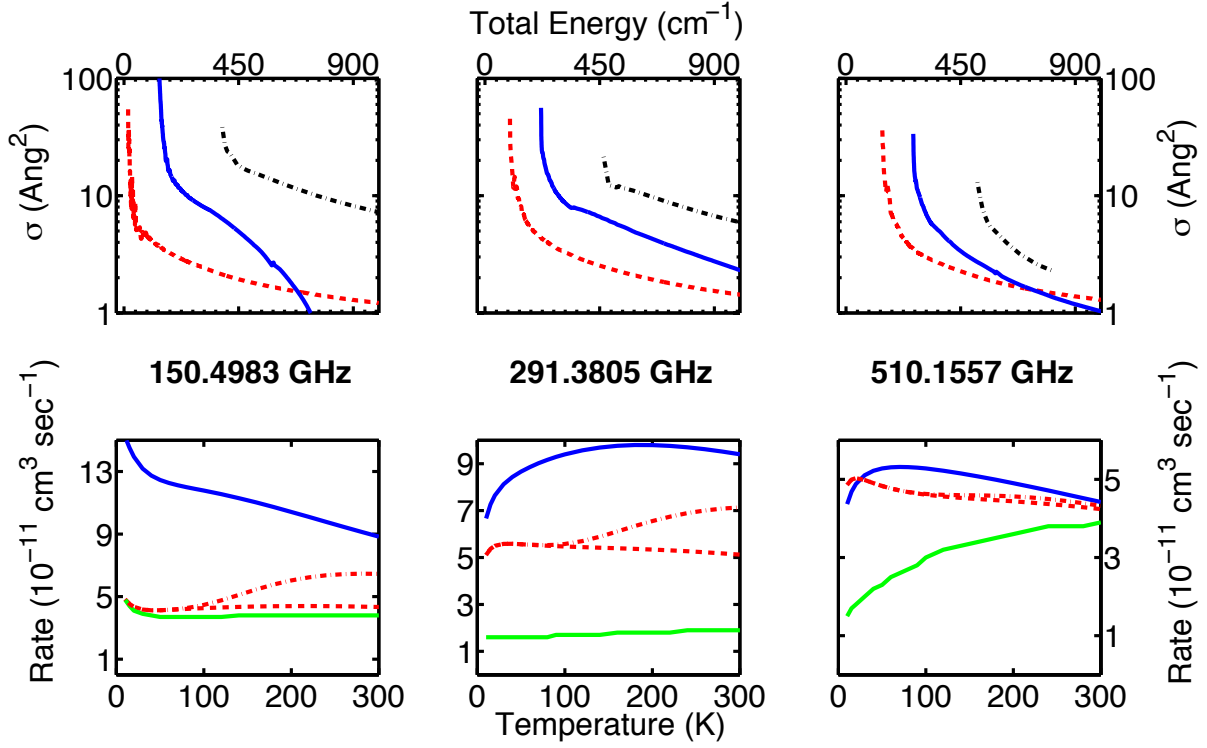


Figure 1. (Color online) Cross-sections (upper three panels) and rates (lower three panels) for three widely observed quenching transitions of ortho- H_2CO (first column : $2_{11} \rightarrow 1_{10}$, at $E_{up} = 22.62 \text{ K}$; second column : $4_{32} \rightarrow 3_{31}$, at $E_{up} = 140.93 \text{ K}$; third column : $7_{35} \rightarrow 6_{34}$, at $E_{up} = 203.9 \text{ K}$). In all panels the red (dashed) line denotes the H_2 rotational $J_2 = 0$ initial and final state, the blue (solid) line, the same with $J_2 = 1$ and the black (dashed-dotted), the same with $J_2 = 2$. The red dash-dotted rates include the influence of the population of the $J_2 = 2$ para state of H_2 (see text). Rates and sections with $J_2 = 0 \leftrightarrow J_2 = 2$ are two or three orders of magnitude lower and not depicted. Rates for collisions with Helium (Green 1991) are the lowest rates in all three inferior panels (green color online). Note that for cross sections, for sake of clarity, the energy is the *total* energy. Note also that cross sections display usual resonance patterns which are not conspicuous at this log scale.

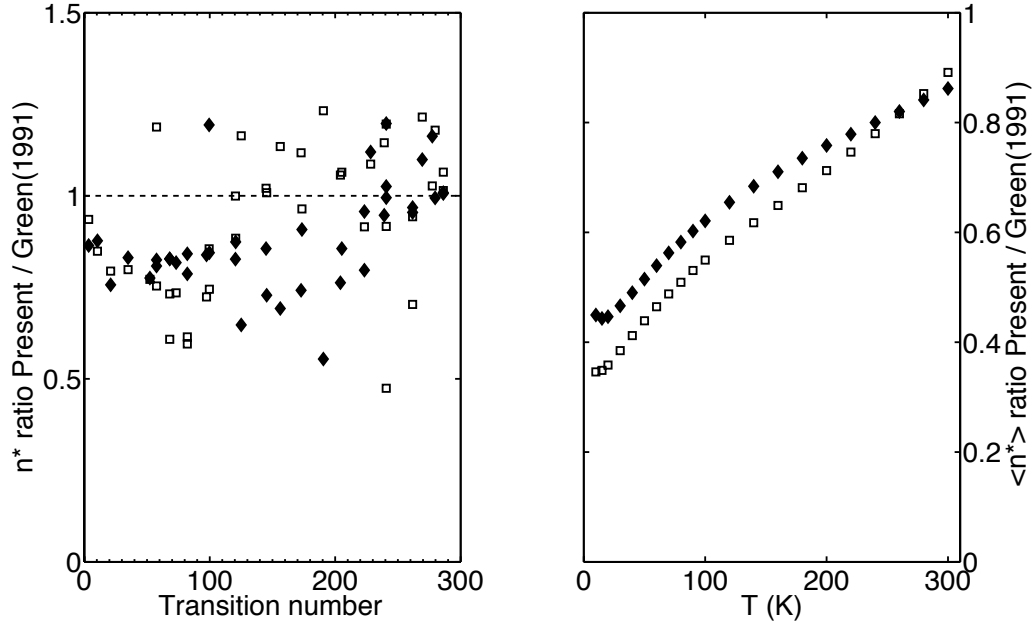


Figure 2. Left panel: ratio of critical densities (eq. 2), present work to Green (1991) properly scaled, for all levels, at $T = 300$ K. Right panel, average over all critical densities ratios, as a function of temperature. Both panels : open squares, ortho-H₂CO with para-H₂ ($J_2 = 0$) or He; filled diamonds para-H₂CO with para-H₂ ($J_2 = 0$) or He.

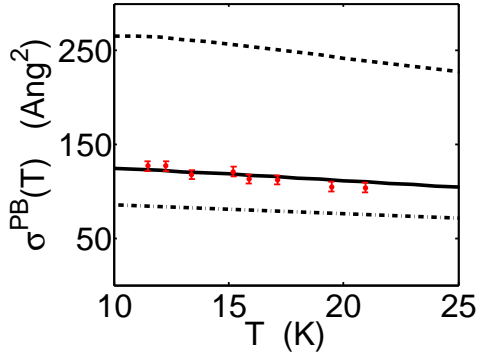


Figure 3. (Color online) Pressure broadening of the $2_{12} \rightarrow 3_{13}$ transition. Red symbols, measurements of Mengel & De Lucia (2000). Dashed and dot-dashed lines, present computations with respectively ortho- H_2 and para- H_2 . Full line, ortho-to-para of H_2 equivalent to a spin temperature of 50 K.